International Journal of ChemTech Research
CODEN (USA): IJCRGG, ISSN: 0974-4290, ISSN(Online):2455-9555
Vol.10 No.10, pp 479-489, 2017

Effect of calcination and sintering temperature on the properties of layered $LiNi_{1/3}Co_{1/3}Mn_{1/3}O_2$ cathode material for lithium-ion batteries

G. Tewodros Aregai[1], K.Vijaya Babu[2]*, B.Vikram Babu[1], V. Veeraiah[1]

[1]Department of Physics, Andhra University, Visakhapatnam-530 003, India
[2]Advanced Analytical Laboratory, Andhra University, Visakhapatnam-530 003, India

Abstract : The layered cathode material for Li-ion batteries was synthesized by solid state reaction method with three step calcination temperatures 500 °C for 5h, 800 °C for 10h, 900 °C for 18h and sintered at 900 °C for 20h. In order to investigate the possible reactions occurring in the synthesis of $LiNi_{1/3}Co_{1/3}Mn_{1/3}O_2$, thermo gravimetric analysis is conducted on the precursor in N_2 atmosphere. The phase composition, micro-morphology, elemental composition and cation distribution of the products are characterized by X-ray diffraction (XRD), scanning electron microscopy (SEM), energy dispersive spectra (EDS) and Fourier transform infrared (FTIR) respectively. The results of XRD pattern possessed the α-$NaFeO_2$ structure of the hexagonal system (space group $R\bar{3}m$). The morphological features of the powders are branded by Scanning electron microscopy (SEM). The FT-IR spectroscopic data reveals that the structure of the oxide lattice constituted by LiO_6, NiO_6, CoO_6 and MnO_6 octahedra. The variation of the ac conductivity, dielectric constant and electric modulus as function of frequency at room temperature (303k) was determined to study the electrical properties of the synthesized samples. From this study, we conclude that the layered $LiNi_{1/3}Co_{1/3}Mn_{1/3}O_2$ material is prepared by solid-state reaction method at different temperature the optimum calcination and sintering temperature is 900^0C for 18h and 900^0C for 20h respectively.
Keywords : Layered structure, XRD, SEM, Impedance, Dielectric constant.

Introduction:

The consideration of advantages and disadvantages of $LiCoO_2$, $LiMnO_2$, and $LiNiO_2$ cathode materials has logically lead to the proposition of the mixed transition metal oxides as the alternative of $LiCoO_2$. Lithium cobalt nickel manganese oxides $LiCo_xMn_yNi_{1-x-y}O_2$ were proposed as possible candidates to replace $LiCoO_2$ cathode [1, 2]. This material adopts the rhombohedral structure of $LiCoO_2$ and $LiNiO_2$. The composition of $LiCo_{1/3}Ni_{1/3}Mn_{1/3}O_2$, referred in the literature as the 333 material [3], contains equal amounts of the transition metals Co, Mn, and Ni; it has high capacity [4] and good rate capability [5]. The lithium removal from the cathode materials leads to the structural changes accompanied by the cell volume change. This volume change could cause the mechanical fracture upon cycling. It was reported that the change in the cell volume for the 333 material $LiCo_xMn_yNi_{1-x-y}O_2$ is about 2%, which is much less than 5% for $LiCo_xNi_{1-x}O_2$ [6], and this small volume change is associated with compensating changes in the *a* and *c* parameters, that is, when the *c* parameter increases, the *a* parameter contracts and vice versa. This may play an important role in the cycle performance improvement of the cathode material. Along with the advantages mentioned above, in its oxidized state $LiCo_{1/3}Ni_{1/3}Mn_{1/3}O_2$ is less oxidative toward the electrolyte than $LiCoO_2$ or $LiNiO_2$ [1]. This material has better

thermal stability than $LiNiO_2$ and shows about 150 and 200 mAh g^{-1} of rechargeable capacity when cycled between 2.5 and 4.3 and 2.5 and 4.6 V, respectively, which makes this cathode more attractive than $LiMn_2O_4$. In $LiCo_{1/3}Ni_{1/3}Mn_{1/3}O_2$the transition metals are in the following oxidation states: Ni (II), Co (III), and Mn (IV). The preparation of an overlithiated material $Li_{1+x}Co_{1/3}Ni_{1/3}Mn_{1/3}O_2$ was shown [7-9] to improve the structure ordering and enhance the cathode cycling and rate capability. Thus, $LiCo_{1/3}Ni_{1/3}Mn_{1/3}O_2$ is considered as a promising next-generation cathode material.

The aim of this work is to synthesized $LiNi_{1/3}Co_{1/3}Mn_{1/3}O_2$ cathode material by solid state reaction method with three step calcination temperatures 500 °C for 5h, 800 °C for 10h and 900 °C for 18h and sintered at 900 °C for 20h. We clarify the effects of calcination and sintering temperature on the of $LiNi_{1/3}Co_{1/3}Mn_{1/3}O_2$ cathode and optimize the calcination and sintering temperature [10].

3. Preparation and experimental techniques:

The cathode compositions are synthesized by a solid-state reaction method from stoichiometric amounts of Li_2CO_3 (Himedia 99.9%), NiO (Himedia 99.9%), Co_2O_3 (Himedia 99.9%) and MnO_2 (Himedia 99.9%).

$$0.5Li_2CO_3 + 1/3NiO + 1/3MnO + 1/6Co_2O_3 \rightarrow LiNi_{1/3}Co_{1/3}Mn_{1/3}O_2 + gas \uparrow$$

A slight excess amount of lithium (5%) was used to compensate for any loss of the metal which might have occurred during the calcination process. The solid state reaction synthesis method involves three steps. First, the precursors, as raw materials, are well mixed and thoroughly ground with agate mortar, then subjected to heat treatment at a temperature of 500 °C for 5 hours and 800 °C for 10 hours to dry the samples free from gases and impurities. Then, this powder was cooled at the rate of 5 °C/ min. Finally, the mixture is reground and calcined at temperatures 900 °C for 18 hours to complete the chemical reaction in air using a muffle box furnace. The powder samples added with polyvinyl alcohol (PVA) as a binder are ground and then pressed at 5 tons / 6 minutes pressure into a circular disk shaped pellet. The pellet is then sintered at 900 °C for 20 h in air at heating and cooling rates of 5 °C/min. The surface layers of the sintered pellet are carefully polished and washed in acetone and then the pellet is coated with silver paste on the opposite faces which act as electrodes.

The TG measurement are conducted using Mettler Toledo TG 851^e instrument from room temperature to 1000 °C in Nitrogen atmosphere at a heating rate of 10 °C /min. The powder X-ray diffraction (XRD) data of the sample is collected on a PANalytical X-pert pro diffractometer with diffraction angles of 10º and 90º in increments of 0.02°. The unit cell lattice parameter is obtained by the unit cell software from the 2θ and (h k l) values. Further, the crystallite size of the sample is obtained by applying the Scherrer's equation from XRD pattern. The particle morphology and elemental analysis of the powders are observed using scanning electron microscopy (SEM) and energy dispersive spectra (EDS) taken from JEOL JSM-6610LV connected with INCA energy 250, Oxford. Fourier transform infrared (FT-IR) spectra are obtained on a Shimadzu IR-Prestige21 spectrometer using KBr pellet technique in the wave number range between 400 and 1400 cm^{-1}.

Results and discussion

Thermal Analysis:

In order to investigate the possible reactions occurring in the synthesis of $LiNi_{1/3}Co_{1/3}Mn_{1/3}O_2$, thermo gravimetric analysis is conducted on the precursor in N_2 atmosphere as shown in figure 1. The weight loss from room temperature to 200 ºC can be assigned to the loss of water adsorbed on the surfaces and some intercalated water molecules and alcohol. In the temperature range of 290-420°C, the weight of the sample decreases quickly, which may result from the complicated reactions of lithium oxide, nickel oxide, cobalt oxide and manganese oxide compounds. The weight of the sample keeps nearly constant in the temperature between 480 °C - 700 °C. The sheer weight loss which occurs between 200 and 600 °C in the curve can be ascribed to the formation of crystalline $LiNi_{1/3}Co_{1/3}Mn_{1/3}O_2$. At higher temperature a weight loss of 3 % between 450 and 500° C has been determined. The transitions at the higher temperatures indicate that these are associated with consolidation and crystallization of the matrices [11, 12].

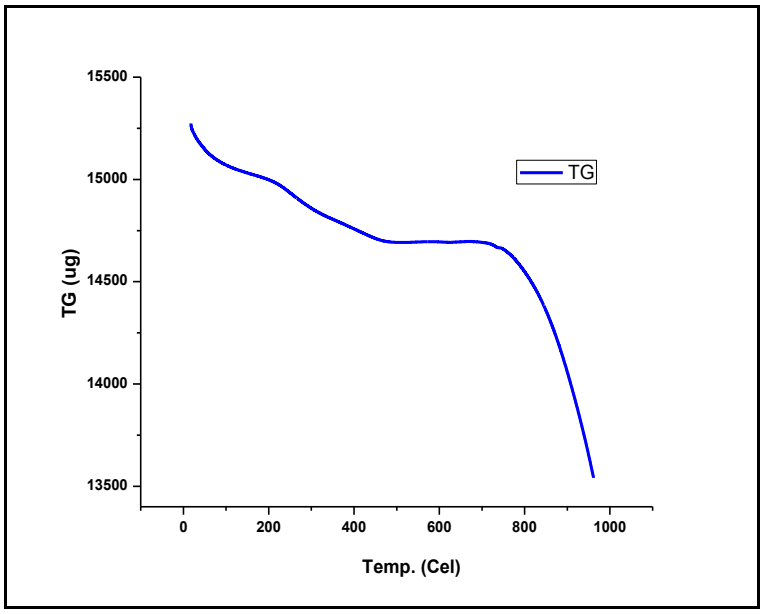

Figure .1 TG curves for $LiNi_{1/3}Co_{1/3}Mn_{1/3}O_2$

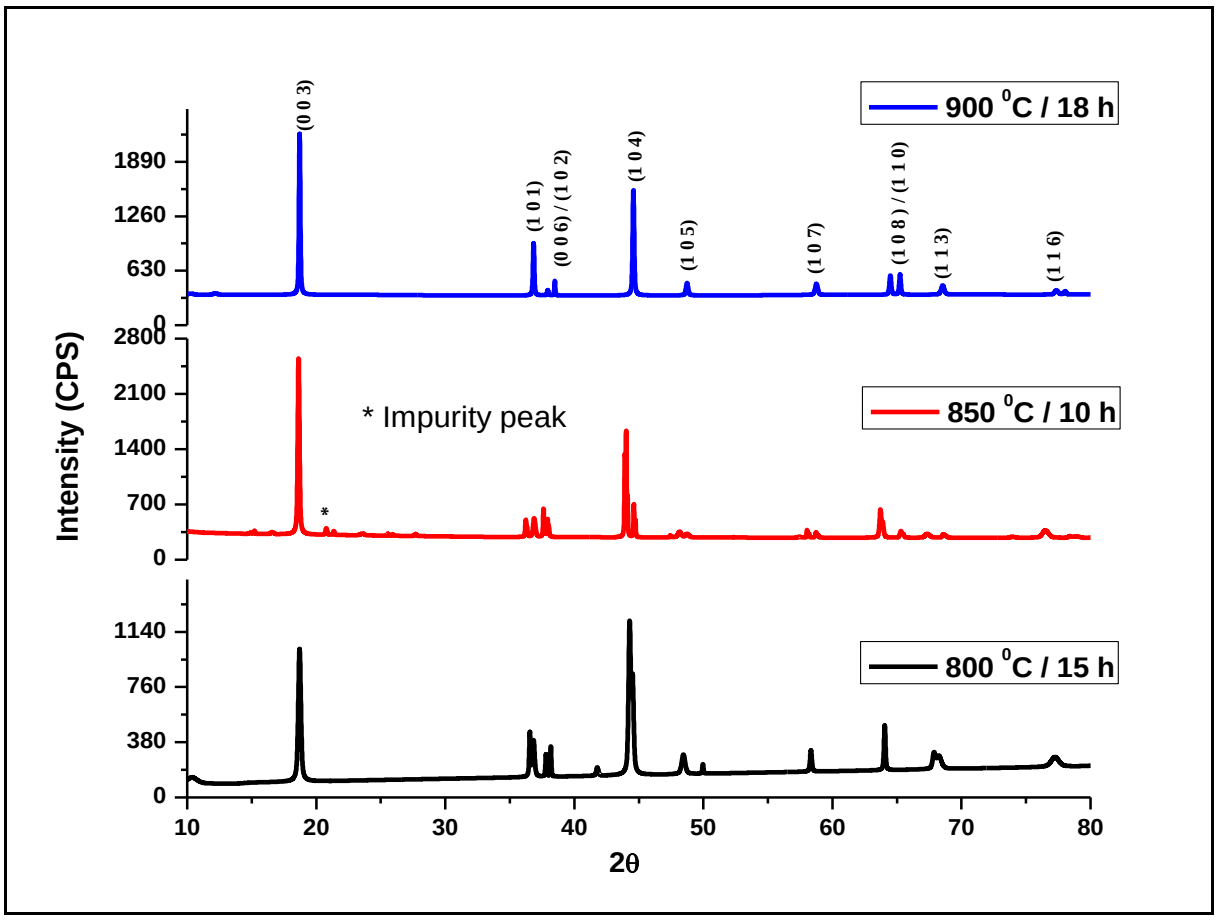

Fig.2 X-ray diffraction patterns of $LiNi_{1/3}Co_{1/3}Mn_{1/3}O_2$ samples synthesized at different temperatures

X-ray Diffraction:

The X-ray diffraction patterns of $LiNi_{1/3}Co_{1/3}Mn_{1/3}O_2$ calcined at different temperatures are shown in figure 2. The XRD patterns of the samples are similar to that of $LiCoO_2$ (α-$NaFeO_2$ type, space group $R\bar{3}m$) and can be indexed as hexagonal lattice. The transition metal atoms (M=Ni, Co, Mn) are supposed to be

randomly distributed on the 3b sites, whereas the lithium atoms occupy the 3a sites and O atoms occupy the 6c sites. No obvious impurity phase peaks can be observed, indicating that the synthesized samples are single phase at 900 °C for 18 hours. In XRD patterns, the splitting of (006)/(102) peak and (108)/(110) peak are regarded as the indications of characteristic of layered structure materials[13]. From the observation of peak splitting of (006)/(102) and (108)/(110) near 38° and 65°, respectively, it can be seen that the layered structure is well developed[14]. The peak splitting in the XRD pattern of $LiNi_{1/3}Co_{1/3}Mn_{1/3}O_2$ synthesized at 900 °C for 18h shows better property indicating that layered structure is better when the calcination temperature is optimal for the formation of pure phase [15, 16].

Table 1: Lattice parameter, unit cell volume, I_{003}/I_{104} and R-factor of $LiNi_{1/3}Co_{1/3}Mn_{1/3}O_2$

Compound	*a* (Å)	c (Å)	V (Å)3	c/*a*	R-factor	I_{003}/I_{104}	Crystallite size (nm)
850 ºC /20h	2.876	14.2997	102.4377	4.9719	0.56	0.8288	82.13
900 ºC /10h	2.851	14.2543	100.3939	4.9984	0.53	1.3175	72.08
900 ºC /18h	2.889	14.367	103.9127	4.9717	0.44	1.52	54.33

The Crystallographic unit cell parameter values deduced through least squares refinement of these XRD pattern(s) yielded cell parameter values a, c, consistent with the literature reports [17] as listed in Table 1. Also turning to growth of particlese-crystallites, some insights become possible with estimate of crystallite size made through Debye- Scherer's. Moreover the observed values of $I_{(003)}/I_{(104)}$ for the synthesized compounds is indicated in the table 1 above. The value of $(I_{006}+I_{102})/I_{101}$ are called R-factor, which is known to be smaller when the hexagonal ordering is high. The R-value is useful to measure the cation disorder. This value is lowest for the synthesized compound and suggests that the hexagonal ordering is better [18-19].The variation of lattice parameter and crystallite size with temperature is presented in figure 3.

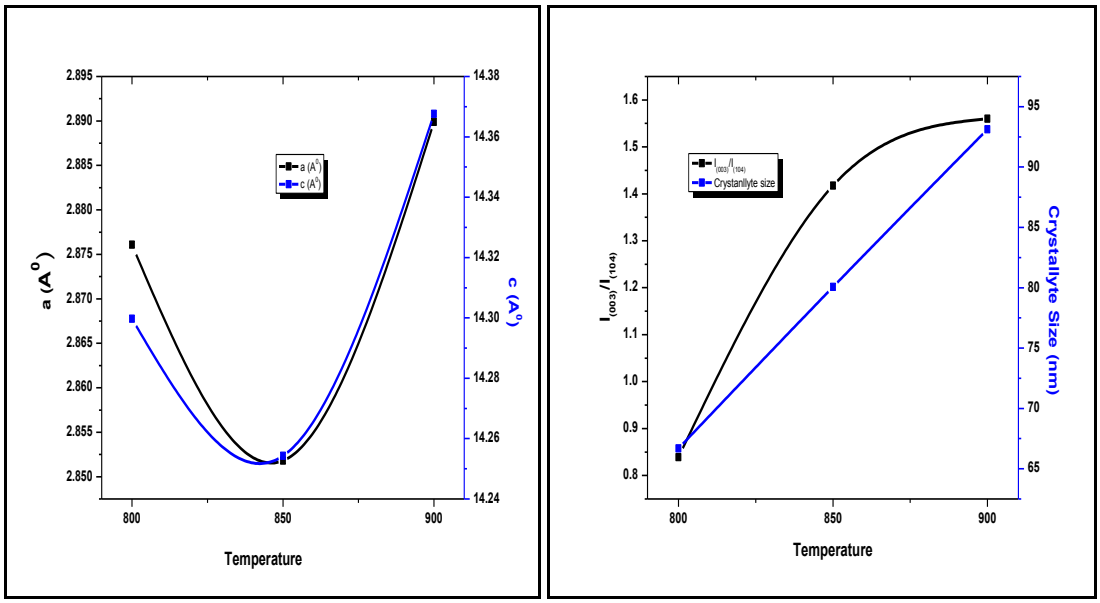

Fig 3: variation of lattice parameter and crystallite size with temperature

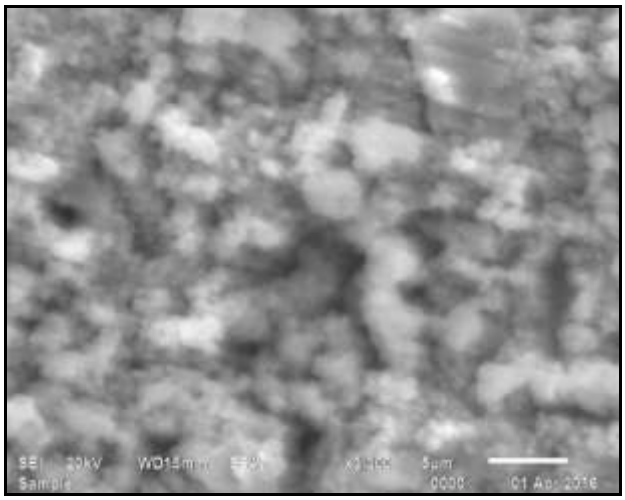

(a)

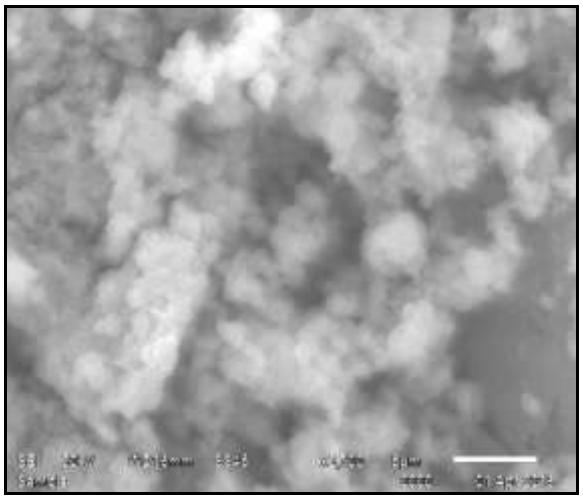

(b)

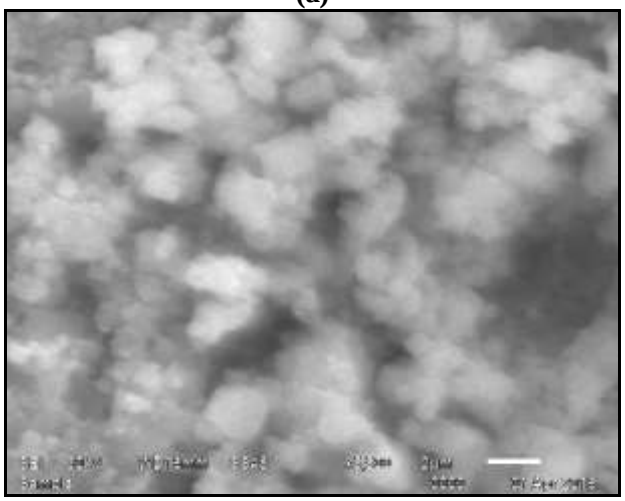

(c)

Fig.4: SEM images of $LiNi_{1/3}Co_{1/3}Mn_{1/3}O_2$ samples calcined at a temperature a) 900° C/18h, b) 850° C/10h and c) 800° C/15h

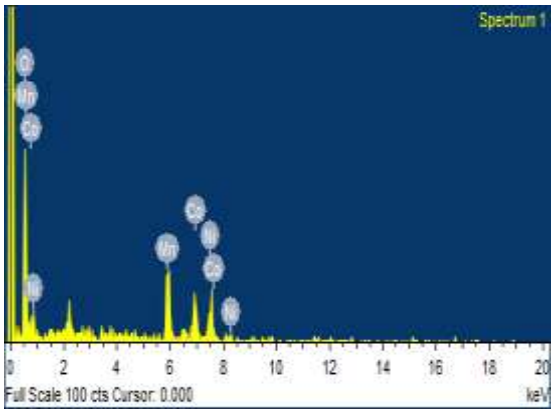

(a)

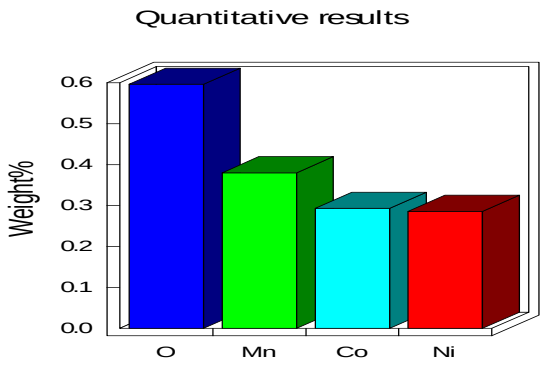

(b)

Element	Weight %	Atomic %
O K	0.60	68.98
Mn K	0.38	12.80
Co K	0.29	9.21
Ni K	0.29	9.01
Totals	1.56	

Fig.5: EDS spectra and quantitative analysis of $LiNi_{1/3}Co_{1/3}Mn_{1/3}O_2$ sample

SEM and EDS

Fig.4. show SEM images for $LiNi_{1/3}Co_{1/3}Mn_{1/3}O_2$ samples calcined at temperatures, 900° C for 18h, 850°C for 10h and 800°C for 15h respectively. The sample calcined at 900° C for 18h have primary particles tend to sinter into tight, smooth particles and the particle size rises and reveals well developed primary particles with quite smooth surface and particle size of 0.5−3μ m. The samples calcined at 850°C for 10h and 800°C for 15h reveal the loose, disordered primary particles.

Fig.5 shows EDS spectra and quantitative analysis of $LiNi_{1/3}Co_{1/3}Mn_{1/3}O_2$ samples calcined at temperatures, 900° C for 18h. The EDS spectra confirmed the presence of Ni, Co, Mn and O in $LiNi_{1/3}Co_{1/3}Mn_{1/3}O_2$ cathode material. It is clearly observed that the spectra show the appropriate ratios of the elements. Lithium is not observed in the EDS spectrum because it has too low of an atomic number to be detected with EDS.

FTIR:

In order to validate the results of XRD analysis, the room temperature FT-IR spectra of the synthesized samples are performed. Fig 6 shows FT-IR spectra of the synthesized sample prepared by solid state reaction method calcined at 900° C/18h. Two distinct peaks are observed in each FT-IR spectrum at different wavelength regions. The two strong frequency bands appeared at wave numbers 603and 545 cm^{-1} are responsible for the formation of $LiNi_{1/3}Co_{1/3}Mn_{1/3}O_2$ which might be attributed to asymmetric stretching modes of Li-M-O.

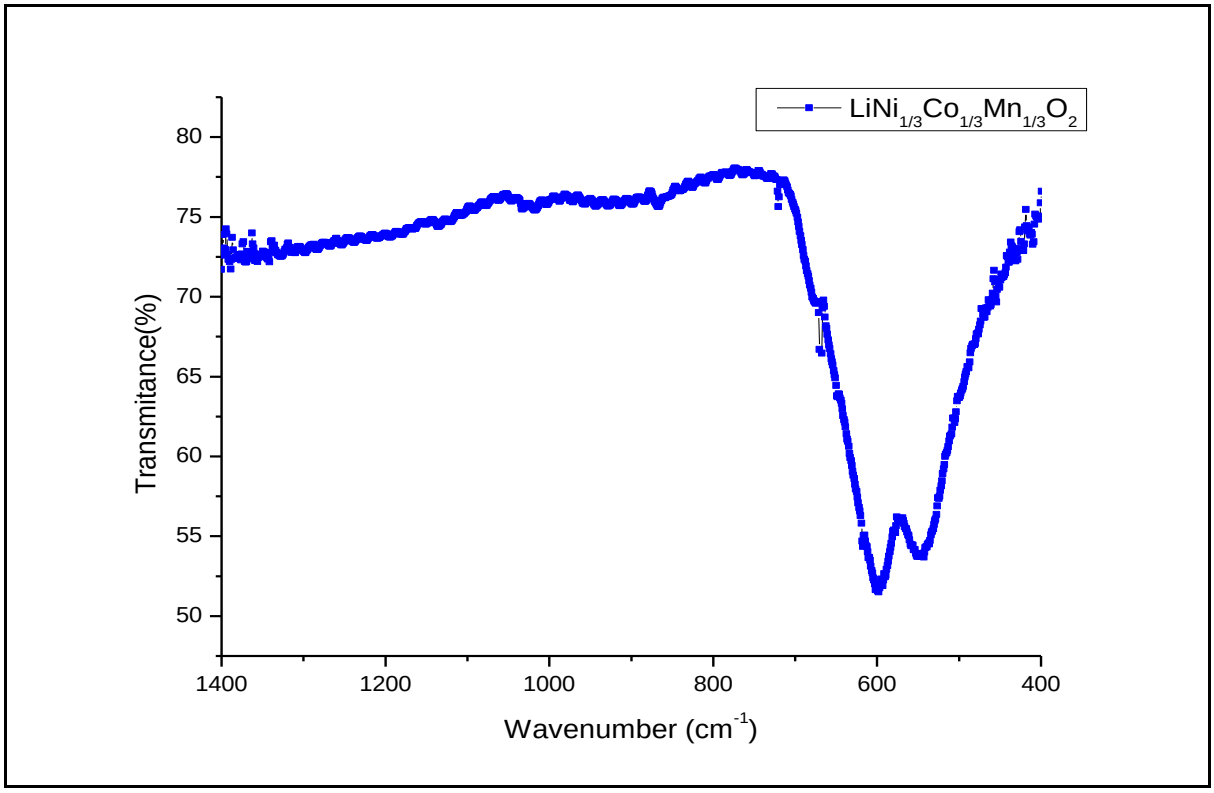

Fig 6: FT-IR spectra of $LiNi_{1/3}Co_{1/3}Mn_{1/3}O_2$ sample calcined at a temperature 900° C/18h

Impedance Analysis:

Electrochemical impedance spectroscopy (EIS) is a powerful tool to identify the kinetics of lithium intercalation/deintercalation into electrode. In general, electrochemical impedance studies are carried out to have better understanding of certain aspects of a lithium cell such as failure mechanism [20], self discharge [21], lithium cycling efficiency [22], interfacial phenomenon between electrode and electrolyte [23] and lithium cation diffusion in the electrode and the electrolyte [24]. Moreover, the EIS measurement technique is also useful to investigate the temperature and frequency dependent behaviour of ac conductivity and dielectric

constant. The obtained results from these analyses can provide information about the electrical behaviour of the samples. Moreover the ac technique has been developed to measure impedance over arrange of frequencies to estimate the exact bulk conductivity and frequency dependant. In the present study, the electrical properties of $LiNi_{1/3}Co_{1/3}Mn_{1/3}O_2$ compound taken at room temperature over the frequency range of 50 Hz to 1 MHz.

Cole-Cole and Bode plots:

Fig. 7 shows the ac Impedance plots of $LiNi_{1/3}Co_{1/3}Mn_{1/3}O_2$ taken at room temperature (303k) for the frequency range 50Hz to 1 MHz. A semicircle was observed on the real axis at the high frequency range. In the low frequency range, a straight line with a certain angle to the real axis corresponds to the Warburg impedance. The high frequency semicircle is related to the charge-transfer resistance and the double-layer capacitance. The low frequency tails resulted from the diffusion of lithium ions in the bulk active mass. In the case of $LiNi_{1/3}Co_{1/3}Mn_{1/3}O_2$ the diameter of the semicircle significantly depends on the potential during charging, indicating that the film formation process is dependent on the lithium ion content. On the other hand, the charge transfer resistance shows a greater dependence on the lithium insertion and extraction levels.

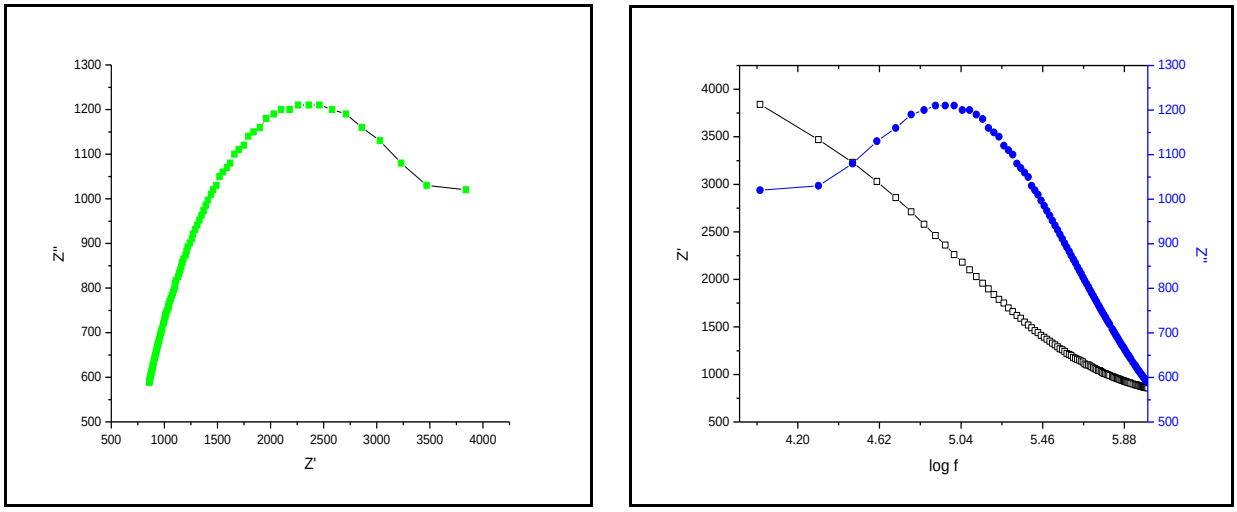

Fig 7: Cole-Cole and Bode plots respectively for $LiNi_{1/3}Co_{1/3}Mn_{1/3}O_2$ samples sintered at a temperature 900° C/20h

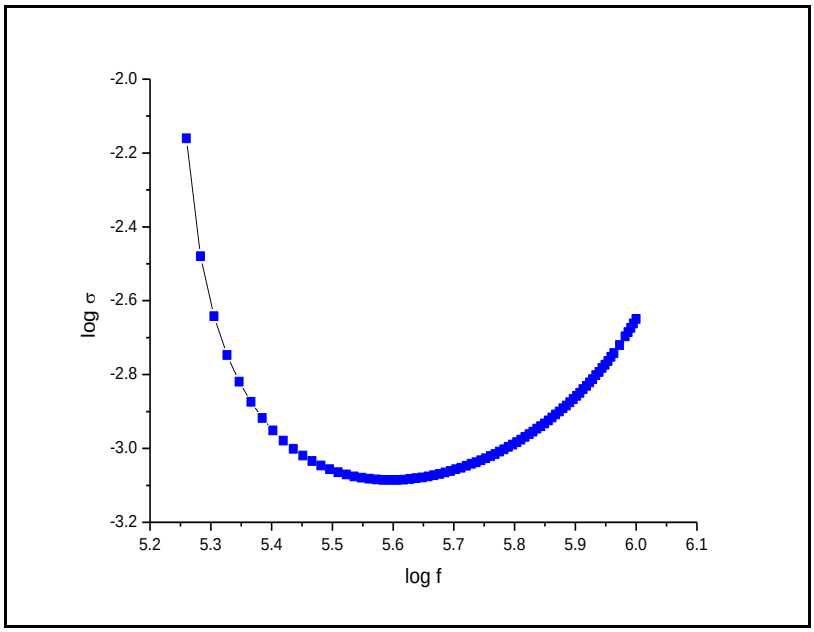

Fig 8 Variation of Conductivity with frequency for LiNi1/3Co1/3Mn1/3O2 samples sintered at a temperature 900° C/20h

Conductivity plots:

The frequency dependence of the conductivity for $LiNi_{1/3}Co_{1/3}Mn_{1/3}O_2$ compound at room temperature for the frequency rang 50 to 1MHz is shown in the fig. 8.

A typical frequency dependence conductivity spectrum exhibit three distinguish regime

a) Low frequency dispersed
b) An intermediate plateau and
c) Conductivity dispersion at high frequency

The variation of conductivity in low frequency region may be attributed to the polarization effects at the electrode interface. At very low frequencies, more charge accumulation occurs and hence, drop in conductivity. In the intermediate frequency region, conductivity is almost found to be frequency independent and at the high frequency region, the conductivity increases with frequency.

Dielectric constant (ε'):

The variation of the dielectric constant (ε') as function of frequency (50 Hz to 1 MHz) at room temperature (303k) for $LiNi_{1/3}Co_{1/3}Mn_{1/3}O_2$ samples is shown in fig.9. From the frequency dependent plot of ε', it is observed that the value of ε' decreases sharply as the frequency increases and attains a constant limiting value, at which ε' becomes almost frequency independent. The higher values of dielectric constant at low frequencies can be due to pile-up of charges at the interfaces between the sample and the electrode. This can be explained based on the behaviour of the dipole movement as follows. Dielectric behaviour of samples with frequency is related to the applied electric field. An alternating electric field changes its direction with time. With each direction reversal, the polarization components are required to follow the field reversal. So, the polarization depends on the ability of dipoles to orient themselves in the direction of the field during each alternative change of the field. At low frequency regions the dipoles will get sufficient time to orient themselves completely along the direction of the field, resulting in larger values of ε' of the samples. As the frequency increases further, the dipoles in the sample cannot reorient themselves fast enough to respond to the applied electric field, resulting in the decrease in ε' of the samples and becoming almost constant.

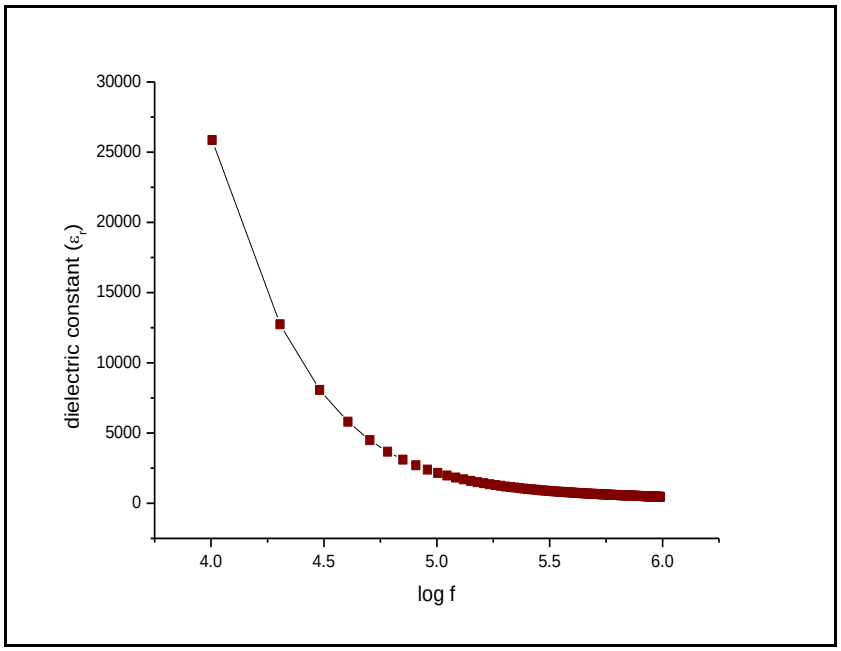

Fig 9 Variation of the dielectric with frequency for LiNi1/3Co1/3Mn1/3O2 samples sintered at a temperature 900° C/20h

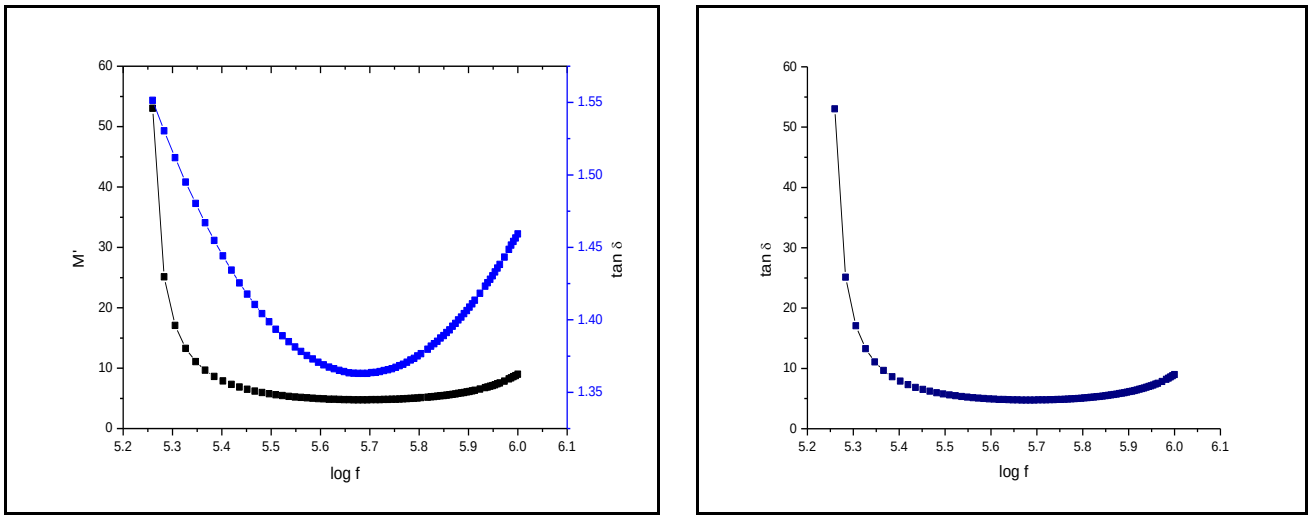

Fig 10 Variation of the dielectric loss (*tanδ)* with the frequency for $LiNi_{1/3}Co_{1/3}Mn_{1/3}O_2$ samples sintered at a temperature 900° C/20h

Dielectric loss (*tanδ*):

The Dielectric loss (*tanδ*) that was ascribed to conduction most probably involves the migration of ions over longer distances. This motion is the same as that occurring under direct current conductions. The variation of the dielectric loss *tanδ* with the frequency at room temperatures is shown in fig.10 for $LiNi_{1/3}Co_{1/3}Mn_{1/3}O_2$. The magnitude of the dielectric loss increases with increase in frequency. At low frequency conduction losses have minimum value. As the frequency increases ac conductivity is also increases, so the conduction losses increase. This leads to increase of the value of *tanδ* with frequency. The increase of the dielectric loss at low frequency is due to dipole polarization.

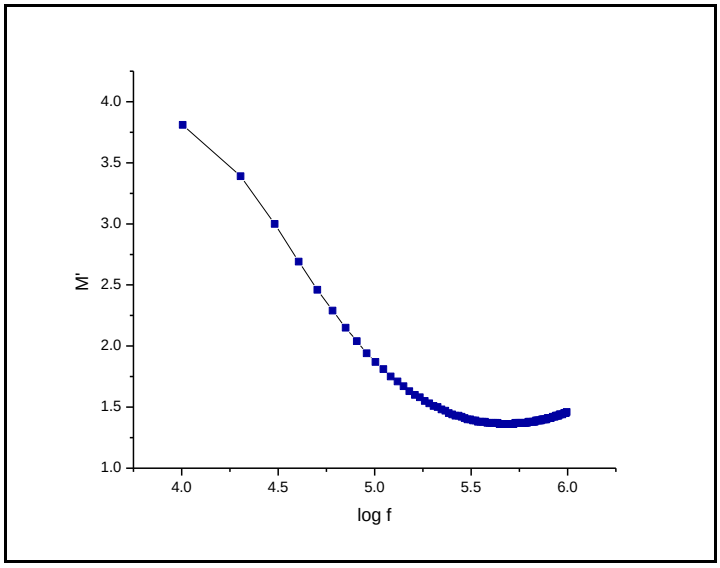

Fig 11: The variation of electric Modulus with frequency for $LiNi_{1/3}Co_{1/3}Mn_{1/3}O_2$ samples sintered at a temperature 900° C/20h

Electric Modulus:

The complex electric modulus spectra represent the measure of the distribution of ion energies or configurations in the structure and also describe the electrical relaxation of ion conducting lattices as a microscopic property of materials [25-28]. The real ($M^{'}$) parts of electric modulus (M*) were calculated using the real part of impedance data measured at different frequencies for $LiNi_{1/3}Co_{1/3}Mn_{1/3}O_2$ sample and pellet dimensions. The variation of the electric modulus as function of frequency (from 50 Hz to 1MHz) at room

temperature (303k) for $LiNi_{1/3}Co_{1/3}Mn_{1/3}O_2$ samples is shown in fig.11 The first one in the low frequency region the electric modulus decreases with frequency and almost frequency independent in the intermediate regions. At higher frequency the value electric modulus increases due to electrical relaxation of ions.

Conclusions:

Layered structure $LiNi_{1/3}Co_{1/3}Mn_{1/3}O_2$ was synthesized by solid state reaction method and effect of calcination and sintering temperature on characteristics of $LiNi_{1/3}Co_{1/3}Mn_{1/3}O_2$ cathode was investigated. In order to investigate the possible reactions occurring in the synthesis of $LiNi_{1/3}Co_{1/3}Mn_{1/3}O_2$, thermo gravimetric analysis is conducted on the precursor in N_2 atmosphere. From X-ray diffraction analysis both the compounds possesses a typical α-$NaFeO_2$ layered structure with $R\bar{3}m$ space group. The SEM morphology shows a very fine surface morphology and the crystal grains. The EDS spectra confirmed the presence of Ni, Co, Mn and O in $LiNi_{1/3}Co_{1/3}Mn_{1/3}O_2$ cathode material. Two distinct peaks are observed in each FT-IR spectrum at different wavelength regions. The two strong frequency bands appeared at wave numbers 603 and 545 cm^{-1} cm^{-1} are responsible for the formation of $LiNi_{1/3}Co_{1/3}Mn_{1/3}O_2$ which might be attributed to asymmetric stretching modes of Li-M-O. The impedance, dielectric, dielectric loss (*tanδ*) and modulus studies of $LiNi_{1/3}Co_{1/3}Mn_{1/3}O_2$ are carried out to study different parameters with frequency and the results are presented. From this study, we conclude that the layered $LiNi_{1/3}Co_{1/3}Mn_{1/3}O_2$ material is prepared by solid-state reaction method at different temperature the optimum calcination and sintering temperature is 900 °C for 18h and 900 °C for 20h respectively.

References:

1. N. Yabuuchi, T. Ohzuku, Novel lithium insertion material of $LiCo_{1/3}Ni_{1/3}Mn_{1/3}O_2$ for advanced lithium-ion batteries, J. Power Sources, 2003, 119-121, 171-174.
2. Y. Chen, G. X. Wang, K. Konstantinov, H. K. Liu, S. X. Dou, Synthesis and characterization of $LiCo_xMn_yNi_{1-x-y}O_2$ as a cathode material for secondary lithium batteries, J. Power Sources, 2003, 119-121, 184-188.
3. E. Zhecheva, R. Stoyanova, Stabilization of the layered crystal structure of $LiNiO_2$ by Co-substitution, Solid State Ionics, 1993, 66, 143-149.
4. Stewart S.G., V. Srinivasan, J. Newman, Modeling the performance of lithium-ion batteries and capacitors during hybrid-electric-vehicle operation, J. Electrochem. Soc. 2008, 155, A664-A671.
5. Martha S.K., H. Sclar, Z.S. Framowitz, D. Kovacheva, N. Saliyski, Y. Gofer, P. Sharon, E. Golik, B. Markovsky, D. Aurbach, A comparative study of electrodes comprising nanometric and submicron particles of $LiNi_{0.50}Mn_{0.50}O_2$, $LiNi_{0.33}Mn_{0.33}Co_{0.33}O_2$ and $LiNi_{0.40}Mn_{0.40}Co_{0.20}O_2$ layered compounds, J. Power Sources, 2009, 189, 248-255.
6. T. Ohzuku, K. Nakumura, T. Aoki, Comparative study of solid-state redox reactions of $LiCo_{1/4}Ni_{3/4}O_2$ and $LiAl_{1/4}Ni_{3/4}O_2$ for lithium-ion batteries, Electrochim. Acta. 1999, 45, 151-160.
7. H. Kobayashi, Y. Arachi, S. Emura, H. Kageyama, K. Tatsumi, T. Kamiyama, Investigation on lithium de-intercalation mechanism for $Li_{1-y}Ni_{1/3}Mn_{1/3}Co_{1/3}O_2$, J. Power Sources, 2005, 146, 640-644.
8. Y. Koyama, N. Yabuuchi, I. Tanaka, H. Adachi, T. Ohzuku, solid-state chemistry and electrochemistry of $LiCo_{1/3}Ni_{1/3}Mn_{1/3}O_2$ for advanced lithium-ion batteries I. first-principles calculation on the crystal and electronic structures, J. Electrochem. Soc. 2004, 151, A1545-A1551.
9. S.H. Park, S.H. Kang, I. Belharouak, Y.K. Sun, K. Amine, Physical and electrochemical properties of spherical $Li_{1+x}(Ni_{1/3}Co_{1/3}Mn_{1/3})_{1-x}O_2$ cathode materials, J. Power Sources, 2008, 177, 177-183.
10. Sathiya. M, A.S. Prakash, K. Ramesha, A.K. Shukla, Rapid synthetic routes to prepare $LiNi_{1/3}Mn_{1/3}Co_{1/3}O_2$ as a high voltage, high-capacity Li-ion battery cathode material, Mater. Res. Bull. 2009, 44, 1990-1994.
11. Caballero. A, M. Cruz, L. Hernan, M. Melero, J. Morales, E.R. Castellon, Nanocrystalline materials obtained by using a simple, rapid method for rechargeable lithium batteries, J. Power Sources, 2005, 150, 192-201.
12. Kamel. K. B, N. Amdouni, A. Abdel-Ghany, K. Zaghib, A. Mauger, F. Gendron, C.M. Julien, Local structure and electrochemistry of $LiNi_yMn_yCo_{1-2y}O_2$ electrode materials for Li-ion batteries, Ionics, 2008, 14, 89-97.

13. Politaev. V.V, A.A. Petrenko, V.B. Nalbandyan, B.S. Medvedev, E.S. Shvetsova, Crystal structure, phase relations and electrochemical properties of monoclinic Li_2MnSiO_4, J. Solid State Chem., 2007, 180, 1045-1050.
14. Youngsik. K, S.K. Hyun, W.M. Steve, Synthesis and electrochemical characteristics of Al_2O_3-coated $LiNi_{1/3}Co_{1/3}Mn_{1/3}O_2$ cathode materials for lithium ion batteries, Electrochimica Acta, 2006, 52, 1316-1322.
15. Dahn. J.R, U. von Sacken, C.A. Michal, Structure and electrochemistry of $Li_{1\pm y}NiO_2$ and a new Li_2NiO_2 phase with the Ni $(OH)_2$ structure, Solid State Ionics, 1990, 44, 87-97.
16. Reimers. J.N, E. Rossen, C.D. Jones, J.R. Dahn, Structure and electrochemistry of $Li_xFe_yNi_{1-y}O_2$, Solid State Ionics, 1993, 61, 335-344.
17. Delmas. C, I. Saadoune, A. Rougier, The cycling properties of the $Li_xNi_{1-y}Co_yO_2$ electrode, J. Power Sources. 1993, 44, 595-602.
18. D'Epifanio. A, F. Croce, F. Ronci, V. Rossi Albertini, E. Traversa and B. Scrosati, Effect of Mg^{2+} Doping on the Structural, Thermal, and Electrochemical Properties of $LiNi_{0.8}Co_{0.16}Mg_{0.04}O_2$, Chem. Mater. 2004, 16, 3559-3564.
19. Pouillerie. C, L. Croguennec, Ph. Biensan, P. Willman, C. Delmas, Synthesis and characterization of new $LiNi_{1-y}Mg_yO_2$ positive electrode materials for lithium-ion batteries, J. Electrochem. Soc. 2000, 147, 2061-2069.
20. Koksbang. R, I. I. Olsen, P. E. Tonder, N.Knudsen, D. Fauteux, Polymer electrolyte lithium batteries rechargeability and positive electrode degradation: An AC impedance study, J.Appl. Electrochem. 1991, 21, 301-307.
21. Pistoia. G, A. Antonin, R. Rosati, D. Zane, storage characteristics of cathodes for li-ion batteries, Electrochim.Acta 1996, 41, 2683-2689.
22. G.Montesperelli, P.Nunziante,M.Pasquili,G.Pistoia, Li passivation in different electrolytes during storage and cycling-An impedance spectroscopy study, Solid State Ionics, 1990, 37, 149-156.
23. Gaberscek. M, S.Pejovnik, Impedance spectroscopy as a technique for studying the spontaneous passivation of metals in electrolytes, Electrochim. Acta 1996, 41, 1137-1142.
24. Capuano.F, F.Croce, B.Scrosati, composite polymer electrolytes, J. Electrochem. Soc., 1991, 138, 1918-1922.
25. Funke. K., Jump relaxation in solid electrolytes, Prog. Solid State Chem. 1993, 22, 111-195.
26. Macedo P.B., C.T. Moynihan and R. Bose, The role of ionic diffusion in polarization in vitreous ionic conductors, Phys. Chem. Glasses, 1972, 13, 171-179.
27. Provenzano.V, L.P. Boesch, V. Volterra, C.T. Moynihan and P.B. Macedo, Electrical Relaxation in Na_2O-$3SiO_2$ Glass. J. Am. Ceram. Soc. 1972, 55, 492-496.
28. Moynihan, C.T., L.P. Boesch and N.L. Laberge, Decay function for the electric field relaxation in vitreous ionic conductors, Phys. Chem. Glasses, 1973, 14, 122-125.

*****